CFD Letters www.cfdl.issres.net Vol. 5 (2) – June 2013

Numerical Modeling of Unequal-size Droplets Collisions using a Lagrangian Mesh-Free Particle Method

Alejandro Acevedo-Malavé*

Centro Multidisciplinario de Ciencias, Instituto Venezolano de Investigaciones Científicas (IVIC), Mérida 5101, Venezuela

Received: 12/10/2012 – Revised 01/06/2013 – Accepted 21/06/2013

Abstract

In this study, a theoretical mesh-free scheme called smoothed particle hydrodynamics (SPH) is employed to resolve the Navier-Stokes equations with the aim to simulate on three dimensional space the coalescence collisions of unequal-size viscous liquid drops. Recently, a SPH scheme has been proposed by Acevedo-Malavé and García-Sucre for the study of collisions between equal-size liquid drops in 3D. This scheme is employed here to model different scenarios for three colliding unequal-size viscous drops. The smoothing length h employed here is a fixed quantity and the smoothing function used is a cubic B-spline kernel. Depending on the velocity of collision, two different outcomes may arise, such as: coalescence and flocculation of drops. It can be seen that when the inertial forces are large enough the coalescence phenomenon is observed, but if the surface tension forces prevailing, the drops tends to form floccs. As a result of the resolution of the Navier-Stokes equations, the velocity vector fields formed inside the drops during the collision process are shown.

Keywords: Drops; Coalescence; Collisions; Fragmentation; Navier-Stokes

1. Introduction

In the literature, the authors propose different methods to approach the dynamics of liquid drops by a numerical integration of the Navier-Stokes equations. These examine the motion of droplets and the dynamics that follows in time and study the liquid bridge that arises when two drops collide. The effects of parameters such as Reynolds number, impact velocity, drop size ratio and internal circulation are investigated and different regimes for droplets collisions are simulated. In some cases, those calculations yield results corresponding to four regimes of binary collisions: bouncing, coalescence, reflexive separation and stretching separation. These numerical simulations suggest that the collisions that lead to rebound between the drops are governed by macroscopic dynamics. In these simulations the mechanism of formation of satellite drops was also studied, confirming that the principal cause of the formation of satellite drops is the "end pinching" while the capillary wave instabilities are the dominant feature in cases where a large value of the parameter impact is employed. Zhang et al. [1] conducted a study on coalescence of unequal-size

* Corresponding Author: Alejandro Acevedo-Malavé Email: alaceved@ivic.gob.ve
 PII: S2180-1363(13)51032-X

drops. In this study, the coalescence of a drop with a flat liquid surface pinches off a satellite droplet from its top, whereas the coalescence of two equally sized drops does not appear to produce in this case a satellite drop. The authors find that the critical ratio grows monotonically with the Ohnesorge number and it is reported the experimental coalescence of two unequal-size droplets. Wang et al. [2] studied the effect of glycerol on the coalescence of water drops in stagnant oil phase. In this reference the authors considered the binary coalescence of water drops formed through capillaries at low inlet flow rates in an immiscible stagnant oil phase. The evolution of the coalescence process is shown in this case. Qian and Law [3] proposed an experimental investigation of binary collision of drops with an emphasis on the transition between different regimes, which may be obtained as an outcome of the collision between droplets. In this study the authors analyze the results using photographic images, which show the evolution of the dynamics exhibited for different values of the Weber number. As a result of the experiment reported by Qian and Law [3], five different regimes governing the collision between droplets are proposed: (i) coalescence after a small deformation, (ii) bouncing, (iii) coalescence after substantial deformation, (iv) coalescence followed by separation in head-on collisions, and (v) coalescence followed by separation in off-center collisions. Foote [4] proposed a method to study the dynamics of liquid drops by a numerical integration of the Navier-Stokes equations. This author examines the motion of droplets with the application to the raindrop problem. The study was restricted to the collision of equal-sized drops along their line of centers. Numerical solutions are developed to study the rebound of water droplets in air. It is found that except for a small viscous effect, the Weber number of the drops determines the dynamics of the collision and the bounce time. Menchaca-Rocha et al. [5] conducted a study on the coalescence and fragmentation of mercury drops of equal and unequal sizes. In this study the authors find out the limits for the coalescence measured in terms of the relative velocity and impact parameter. Experimental studies of the binary collision of alkane droplets were carried out by Ashgriz and Givi [6,7]. These authors found that when the Weber number is increased, the collision takes a high-energy form and different types of results arises. In these references the results show that the collision of the droplets can be bouncing, grazing and generating satellite drops. A similar experimental study about binary collision of equal-size alcohol droplets has been carried-out by Brenn and Frohn [8], showing different stages of the collision process. Podgorska [9] reported experimental studies on the coalescence of toluene as well as silicone oil drops of different viscosities and the results of model predictions. The coalescence model was based on the assumption of partially mobile drop interfaces and has been applied for toluene as well as for silicone oil. Three different models for immobilized drop interfaces were proposed for silicone oil of high viscosity. Drop size distributions were predicted by solving the population balance equation with the assumption of partial mobility. This approach yields good results for toluene and quite good ones for silicone oil of low viscosity. For silicone oil of high viscosity, drop size distribution cannot be precisely predicted by simple models because drops of different sizes behave in completely different ways. However, the proposed models allow the discussion of the experimental observations. Roisman et al. [10] studied the collisions of liquid drops dominated by inertial forces. They compare the experimental data with numerical simulations for the shape of the lamella that is generated by the impact of the droplets. The results show that for Reynolds number and Weber number high enough, the evolution of the lamella thickness is independent of the viscosity and surface tension. Sun et al. [11] conducted a study of deformation and mass transfer for binary droplet collisions with the moving particle semi-implicit method. A surface tension model is implemented in numerical simulations to study large deformation processses, and a mechanism map is reported to distinguish different collisions regimes. Eggers et al. [12] conducted a study about the dimensions of the bridge that arises when two droplets collide to form a bigger drop. In this study the authors conclude that the analyzed problem is asymptotically equivalent to the two-dimensional problem. These authors also studied analytically and numerically the case of coalescence of drops in the presence of an external viscous fluid, finding a toroidal structure. Ashgriz and Poo [13] conducted an experimental study of the binary collision of water droplets for a wide range of Weber

numbers and impact parameters. These authors identified two types of collisions leading to the separation of drops, which can be reflexive separation and stretching separation. It is found that the reflexive separation occurs in head-on collisions, while stretching separation occurs in high values of the impact parameter. Experimentally, the authors report the border between the two types of separation, and also collisions that lead to coalescence. Rekvig and Frenkel [14] reported a molecular simulation study of the mechanism of droplets covered with surfactant monolayer coalescence. The authors proposed a model system where the rate-limiting step in coalescence is the rupture of the surfactant film. For this numerical study one of the authors made use of the dissipative particle dynamics method using a coarse-grained description of the oil, water, and surfactant molecules. The authors find that the rupture rate is highest when the surfactant has a negative natural curvature, and lowest when it has a zero natural curvature, and lying in between when it has a positive natural curvature. Thoroddsen et al. [15] conducted an experimental study of surface profiles and the propagation of Marangoni waves along the surface of a drop. It can be found that the capillary-Marangoni waves along the water drop show self-similar characteristics when measured in terms of the arc length of the original surface. The coalescence for different liquids was also studied, finding that the coalescence velocity of a water drop with a more viscous liquid is nearly independent of the viscosity difference strength. Mashayek et al. [16] studies the coalescence collision of two liquid drops using a Galerkin finite element method in conjunction with the spine-flux method for the free surface tracking. The effects of some parameters, like Reynolds number, impact velocity, drop size ratio, and internal circulation on the coalescence process, are investigated. The long time oscillations of the coalesced drops and the collision of unequal-size liquid drops are studied to illustrate the liquid mixing during the collision. Xing et al. [17] put forward a lattice Boltzmann method-based-single-phase free surface model to study the interfacial dynamics of coalescence, droplet formation and detachment phenomena related to surface tension and wetting effects. A perturbation similar to the first step in Gunstensen's color model is added to the distribution functions of the interface cells in order to incorporate the surface tension into the single-phase model. Implementations of the model are verified, simulating the processes of droplet coalescence, droplet formation and detachment from ceiling and from nozzles with different shapes and different wall wetting properties. Acevedo-Malavé and García-Sucre [18] study the coalescence collision between two equal-size liquid drops. In this work the authors report a three dimensional collisions of drops. When the inertial forces are large enough, the droplet collisions tends to form a bigger number of satellite drops at the zone of contact between the drops and the end pinching mechanism is described. If the inertial forces are too low the surface tension forces prevailing and the drops form a flocc.

In this study, the interaction between three unequal-size drops is studied. The aim of this paper is to show the modeling of the coalescence process using the Smoothed Particle Hydrodynamics method. This method is used to solve the equations of fluid dynamics using a set of particles that interacts between them depending on the value for the smoothing length h. The model reported in this paper is performed in 3D and it is used the cubic B-spline kernel Monaghan [19]. In this work water drops are considered.

2. Numerical details

2.1. The Smoothed Particle Hydrodynamics method

Smoothed Particle Hydrodynamics is a method to solve approximately the equations of fluid dynamics, replacing the fluid by a set of particles. The SPH method was simultaneously invented by Lucy [20] and Gingold and Monaghan [21] to solve astrophysical problems.

In the SPH model, the fluid is represented by a discrete set of N particles. The position of the ith particle is denoted by the vector r_i, i=1,…, N. The SPH scheme is based on the idea that a

smoothed representation $A_s(r)$ of the continuous function A(r) can be obtained from the convolution integral

$$A_s(\mathbf{r}) = \int A(\mathbf{r}')W(\mathbf{r}-\mathbf{r}',h)d\mathbf{r}'. \quad (1)$$

Here h is the smoothing length, and the smoothing function W satisfies the normalization condition

$$\int W(\mathbf{r}-\mathbf{r}',h)d\mathbf{r}' = 1. \quad (2)$$

The integration is performed over all spaces. In the limit of h tending to zero, the smoothing function W becomes a Dirac delta function, and the smoothed representation $A_s(r)$ tends to A(r).

In the SPH scheme, the properties associated with particle i, are calculated by approximating the integral in eq. (1) by the sum

$$A_i = \sum_j \Delta V_j A_j W(\mathbf{r}_i - \mathbf{r}_j, h) = \sum_j m_j \frac{A_j}{\rho_j} W(\mathbf{r}_i - \mathbf{r}_j, h). \quad (3)$$

Here ΔV_j is the fluid volume associated with particle j, and m_j and ρ_j are the mass and density of the jth particle, respectively. In the above sum, A_j is the value of a physical field A(r) in the particle j, and the sum is performed over all particles. Furthermore, the gradient of A is calculated using the expression

$$\nabla A_i = \sum_j m_j \frac{A_j}{\rho_j} \nabla_i W(\mathbf{r}_i - \mathbf{r}_j, h). \quad (4)$$

In the equation (3), ρ_i/m_i can be replaced by the particle number density $n_i=\rho_i/m_i$, so that

$$A_i = \sum_j \frac{A_j}{n_j} W(\mathbf{r}_i - \mathbf{r}_j, h). \quad (5)$$

The particle number density can be calculated using the expression

$$n_i = \sum_j W(\mathbf{r}_i - \mathbf{r}_j, h), \quad (6)$$

and the mass density is given by

$$\rho_i = \sum_j m_j W(\mathbf{r}_i - \mathbf{r}_j, h). \quad (7)$$

Similarly, the gradient can be calculated using the expression

$$\nabla A_i = \sum_j \frac{A_j}{n_j} \nabla_i W(\mathbf{r}_i - \mathbf{r}_j, h). \tag{8}$$

The velocity and acceleration fields are given by [18]

$$\frac{d\mathbf{r}_i}{dt} = \mathbf{v}_i, \qquad \frac{d\mathbf{v}_i^{\alpha}}{dt} = \sum_{j=1}^{N} m_j \left(\frac{\sigma_i^{\alpha\beta}}{\rho_i^2} + \frac{\sigma_j^{\alpha\beta}}{\rho_j^2} \right) \cdot \nabla W_{ij}^{h}, \tag{9}$$

where σ is the total stress tensor.

The internal energy evolution is given by the expression [18]

$$\frac{dE_i}{dt} = \frac{1}{2} \sum_{j=1}^{N} m_j \left(\frac{p_i}{\rho_i^2} + \frac{p_j}{\rho_j^2} \right) \left(\mathrm{v}_\mathrm{i}^{\beta} - \mathrm{v}_j^{\beta} \right) \frac{\partial W_{ij}}{\partial x_i^{\beta}} + \frac{\mu_i}{2\rho_i} \varepsilon_i^{\alpha\beta} \varepsilon_i^{\alpha\beta}, \tag{10}$$

In the above equation p is the pressure, μ is the dynamic viscosity and ε is the shear strain rate.

In the present work, the model is performed in three dimensions and the cubic B-spline kernel is used [19]. In this paper, water drops are considered and the equation of state in the hydrodynamical code was a general Mie-Gruneisen form of equation of state with different analytic forms for states of compression ($\rho/\rho 0-1$)>0 and tension ($\rho/\rho 0-1$)<0 [18].

This equation has several parameters, namely the density ρ, the reference density ρ_0, and the constants A_1, A_2, A_3, C_1 and C_2. This equation of state defines the pressure P as

$$P = A_1 \left(\frac{\rho}{\rho_0} - 1 \right) + A_2 \left(\frac{\rho}{\rho_0} - 1 \right)^2 + A_3 \left(\frac{\rho}{\rho_0} - 1 \right)^3 \quad if \quad \left(\frac{\rho}{\rho_0} - 1 \right) > 0 \tag{11}$$

and

$$P = C_1 \left(\frac{\rho}{\rho_0} - 1 \right) + C_2 \left(\frac{\rho}{\rho_0} - 1 \right) \quad if \quad \left(\frac{\rho}{\rho_0} - 1 \right) < 0. \tag{12}$$

In all calculations the following values are used for the constants: $A_1=2.20\text{x}10^6$ kPa, $A_2=9.54\text{x}10^6$ kPa, $A_3=1.46\text{x}10^7$ kPa, $C_1=2.20\text{x}10^6$ kPa, $C_2=0.00$ kPa, and $\rho_0=1000.0$ Kg/m^3.

3. Results and discussion

In order to simulate the hydrodynamical coalescence collisions between three unequal- size water drops, the Smoothed Particle Hydrodynamics formalism has been employed. Inside the SPH code were defined drops with 10 μm, 16 μm and 30 μm of diameter and 26656 SPH particles for the three drops with a collision velocity of 15.0 mm/ms directed to the center of the coordinate system.

It can be seen in figure 1 that at $t=1.1\text{x}10^{-4}$ ms a flat circular section appears, which increases its diameter as dynamics progresses. It is observed in the dynamics that at $t=1.5\text{x}10^{-4}$ ms a bridge structure between the drops appears in the region of contact, which disappears at a later time due to the penetration of SPH particles between the drops. After a process of

coalescence occurs (see figure 1 at $t=2.0x10^{-4}$ ms), a bigger mass of liquid is formed (see this figure at $t=2.8x10^{-4}$ ms). Figure 2 shows the velocity vector field inside the droplets as well as in the region of contact between them at $t=2.0x10^{-4}$ ms. It is important to see that inside the drops, the fluid tends to a velocity value around the initial velocity of 15.00 mm/ms, while in the area of contact between the drops an increase in the fluid velocity to a value of 30.0 mm/ms is observed. This increase in the fluid velocity is due to changes on the pressure field inside the drops. In fact, in the region of contact of the droplets, the value of pressure reaches its maximum value.

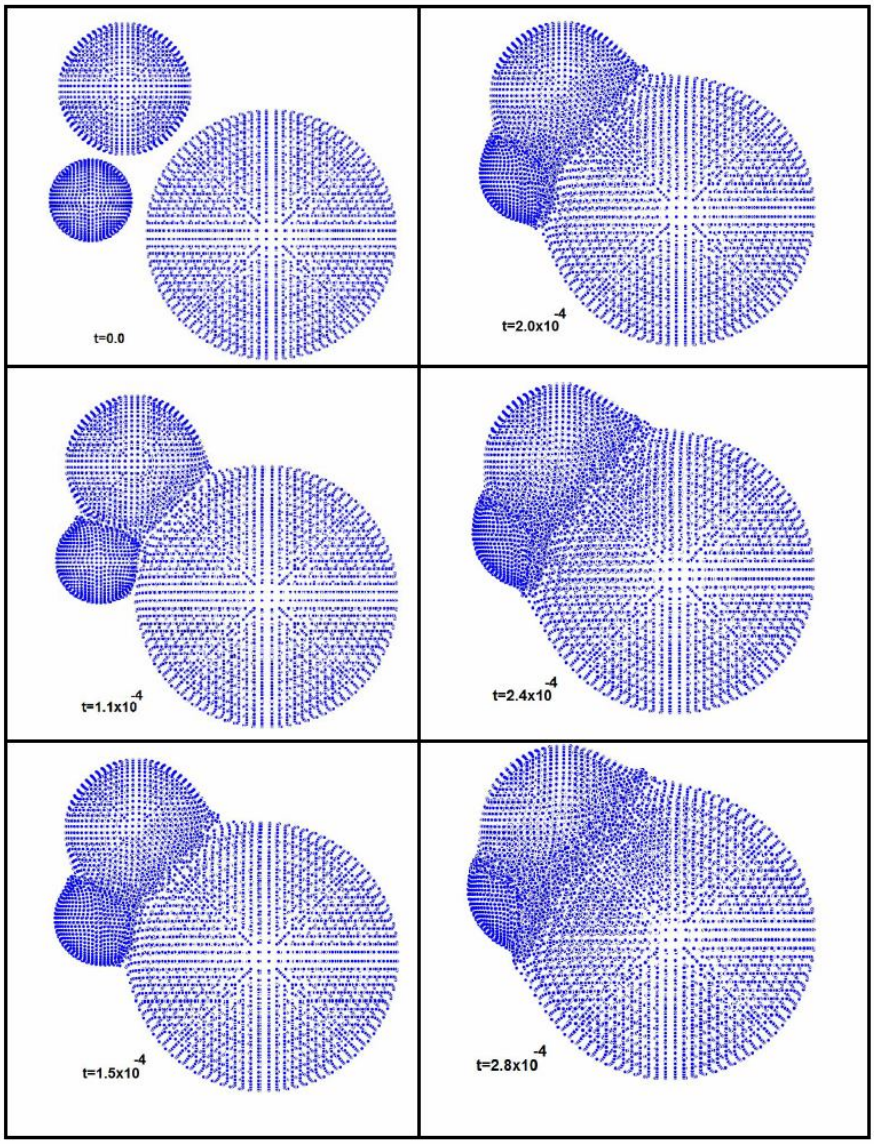

Figure 1. Sequence of times showing the evolution of the collision between three drops (permanent coalescence) with V_{col} = 15.0 mm/ms. The evolution of time is given in milliseconds.

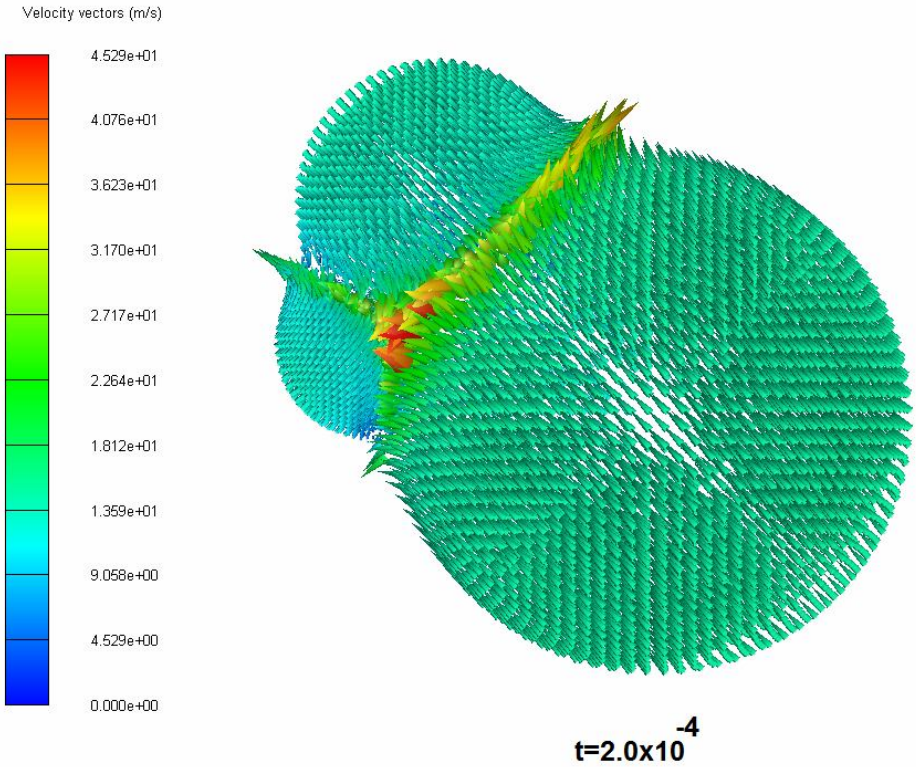

Figure 2. Velocity vector field for the collision between three drops at $t=2.0x10^{-4}$ ms (permanent coalescence) with V_{col}=15.0 mm/ms. The evolution time is given in milliseconds.

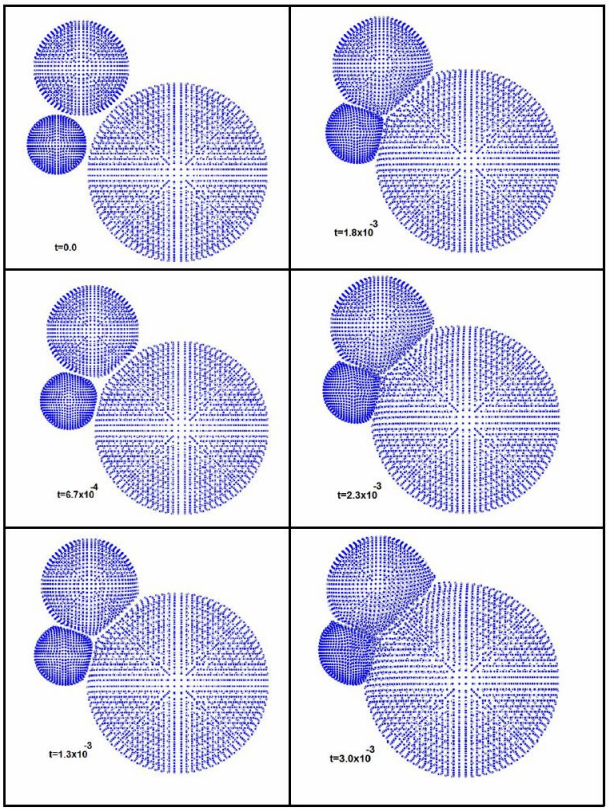

Figure 3. Sequence of times showing the evolution of the collision between three drops (flocculation) with V_{col}=0.5 mm/ms. The evolution of time is given in milliseconds.

Flocculation occurs when the collision velocity is decreased below the range corresponding to permanent coalescence. These calculations were performed for droplets with 10 µm, 16 µm and 30 µm of diameter and 26656 SPH particles for the three drops with a collision velocity of 0.5 mm/ms directed to the center of the coordinate system. At the beginning of the calculation it can be observed at $t=6.7x10^{-4}$ ms (see figure 3) that a flat circular section appears between the three droplets, which at $t=1.3x10^{-3}$ ms has already increased in diameter. As the dynamics run a stretching of the surface of the drops until $t=3.0x10^{-3}$ ms can be observed and the droplets form a floc. Figure 4 shows the velocity vector field at $t=2.0x10^{-3}$ ms in the flocculation process. As shown in figure 4, the fluid velocity inside the drops is around 0.65 mm/ms and at the zone of contact of the droplets the velocity is around 0.85 mm/ms.

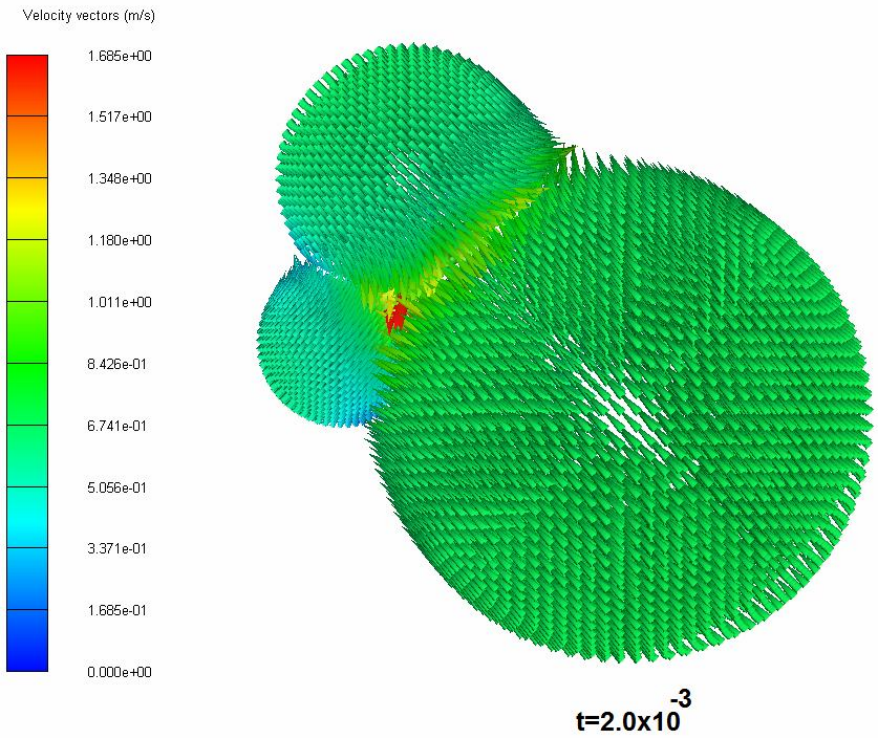

Figure 4. Velocity vector field for the collision between three drops at $t=2.0x10^{-3}$ ms (flocculation) with $V_{col}=0.5$ mm/ms. The evolution time is given in milliseconds.

In order to simulate the fragmentation phenomenon, Inside the SPH code were defined drops with 10 µm, 16 µm and 30 µm of diameter and 26656 SPH particles for the three drops with a collision velocity of 30.0 mm/ms directed to the center of the coordinate system.With this value for the velocity of collision it is observed that the fragmentation phenomenon arises, i.e. the regime 2 reported by \citep{Qian97}[4] occurs giving rise to coalescence followed by separation into small satellite drops. In the first stage of the calculation at $t=3.7x10^{-5}$ ms the collision of the three droplets is shown in figure 5. It can be seen the formation of a flat circular section between the drops. This circular section vanishes completely at $t=1.7x10^{-4}$ ms. At this time a portion of fluid appears to form a wave front propagating in the three-dimensional space. This wave front begins to form little satellite drops and increases its amplitude. There is no substantial growth of these satellite drops and the structure tends to a bell form as the dynamic runs. Figure 6 shows the velocity vector field after the fragmentation of the drops has taken place. As shown in figure 6, the fluid velocity inside the drops is 27 mm/ms, which is less than the initial rate of collision, while the fluid that is spread to the edges is accelerated reaching a speed of 60.0 mm/ms. A longer stretched ligament is produced and the amount of satellite droplets increases with the evolution of dynamics. Figure 5 illustrates

that a small portion of the fluid begins to separate, stretching away from the bigger drop, and a non-uniform pressure field is created inside the ligament. This is related to the value in the velocity vector field differences. Once the ligament begins to form (see figure 5), a flow is generated directed in the opposite direction. This motion transform this portion of the ligament in a bulbous due to the accumulation of mass in this volume, and this change in geometry implies the appearance of a local minimum in the pressure field which is located between the bulbous and its neighboring region.

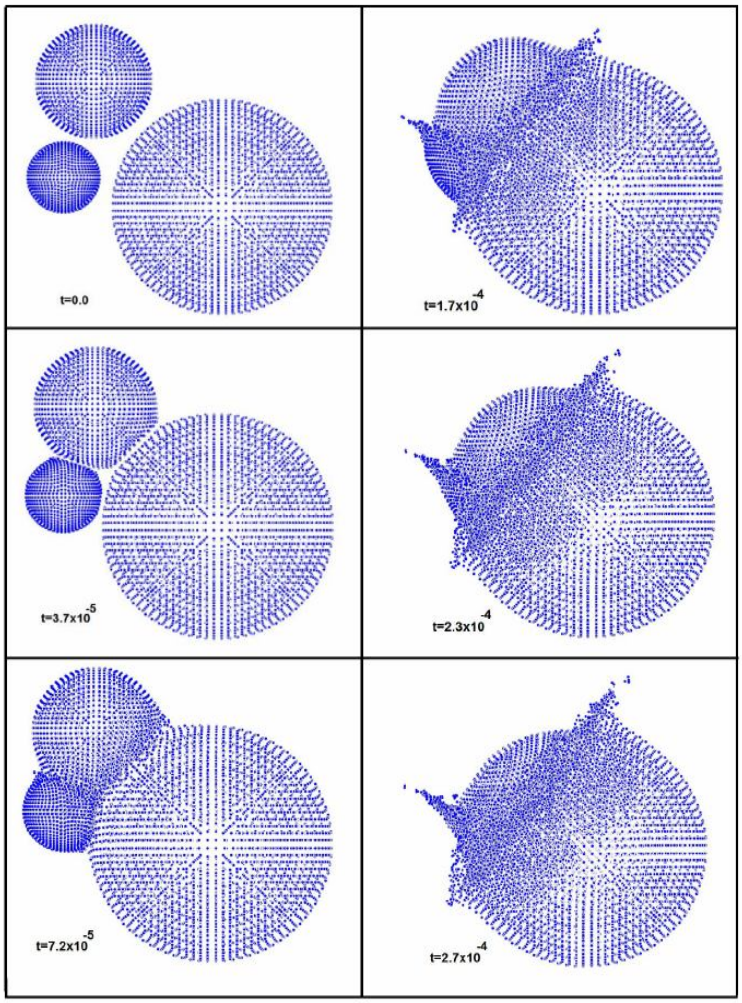

Figure 5. Sequence of times showing the evolution of the collision between three drops (fragmentation) with V_{col}=30.0 mm/ms. The evolution of time is given in milliseconds.

As a result of this pressure difference a local flow is generated through the point of minimum pressure that opposes to the flow that is coming from the bulbous. This fluid motion causes a local reduction of mass and therefore the ligament between the bulbous and the neighboring region starts to decrease its radius (at the point of minimal pressure). Because of this local decrease of the ligament radius the pressure rises, which creates a flow with the same direction of the flow that comes from the end of the bulbous and other flow in the opposite direction from the point of local reduction of mass. Given these opposing flows emerging from this point, the radius of the ligament decreases even more. Then the system tends to relax this unstable situation reducing the radius of this region to zero, giving rise to a division of the fluid and so producing a satellite drop (see figure 5). Subsequently, this process is repeated in the other regions of the ligament, producing more satellites drops. These shattering collisions occur only at high velocities making the surface tension forces of secondary importance (the phenomenon is inertial dominated).

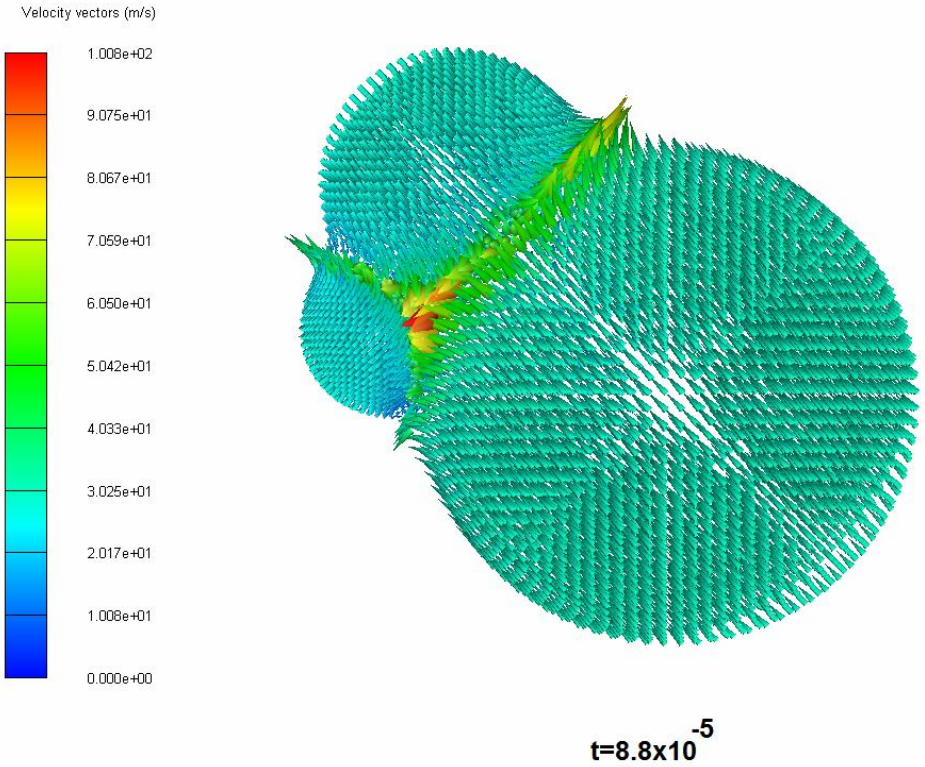

Figure 6. Velocity vector field for the collision between three drops at $t=8.8x10^{-5}$ ms (fragmentation) with $V_{col}=30.0$ mm/ms. The evolution time is given in milliseconds.

4. Conclusion

An adequate methodology has been proposed for the modeling of hydrodynamical collisions between liquid drops using the SPH formalism in three-dimensional space. Two scenarios for the collisions of liquid drops in three dimensions have been carried out in the simulations. A flat circular section arises as the initial stage in all SPH calculations reported in this work. This flat circular section appears due to the existence of surface tension forces acting on each droplet. A range of values for the collision velocity is chosen and the possible outcomes for the collision process are obtained: coalescence and flocculation of drops. The velocity vector fields were constructed by different calculations. It can be seen that the fluid inside the drops tends to accelerate the SPH particles at the zone of contact between the droplets. This behavior is due to the non-uniform pressure differential inside the drops. At the zone of the drops which have no interaction with any other drop, the fluid tends to diminish the internal velocity. This can be explained by the behavior of the pressure field inside the drops, in fact, in that zone of the droplets, the inhomogeneous pressure field has a minimal value.

REFERENCES

[1] Zhang, F. H., Li, E. Q. and Thoroddsen, S. T., *Satellite formation during coalescence of unequal size drops*. Phys. Rev. Lett., 2009. **102**: p. 1-4.

[2] Wang, W., Gong, J., Ngan, K. H. and Angeli, P., *Effect of glycerol on the binary coalescence of water drops in stagnant oil phase.* Chem. Eng. Res. Design, 2009. **87**: p. 1640-1648.

[3] Qian, J. and Law, C. K., *Regimes of coalescence and separation in droplet collision.* J. Fluid Mech., 1997. **331**: p. 59-80.

[4] Foote, G. B., *The water drop rebound problem: Dynamics of collision*. J. Atmos. Sci., 1974. **32**: p. 390-401.
[5] Menchaca-Rocha, A., Huidobro, F., Martinez-Davalos, A., Michaelian, K., Perez, A., Rodriguez, V. and Carjan, N., *Coalescence and fragmentation of colliding mercury drops.* J. Fluid Mech., 1997. **346**: p. 291-318.
[6] Ashgriz, N. and Givi, P., *Binary collision dynamics of fuel droplets.* Int. J. Heat Fluid Flow, 1987. **8**: p. 205-208.
[7] Ashgriz, N. and Givi, P., *Coalescence efficiencies of fuel droplets in binary collisions*. Int. Commun. Heat Mass Transfer, 1989. **16**: p. 11-17.
[8] Brenn, G. and Frohn, A., *Collision and merging of two equal droplets of propanol*. Exp. Fluids, 1989. **7**: p. 441-446.
[9] Podgorska, W., *Influence of Dispersed Phase Viscosity on Drop Coalescence in Turbulent Flow.* Chem. Eng. Res. Design, 2007. **85**: p. 721-729.
[10] Roisman, L., Berberovic, E. and Tropea, C., *Inertia dominated drops collisions. I. On the universal flow in the lamella.* Phys. Fluids, 2009. **21**: p. 1-10.
[11] Sun, Z., Xi, G. and Chen, X., *Mechanism study of deformation and mass transfer for binary droplet collisions with particle method.* Phys. Fluids, 2009. **21**: p. 1-13.
[12] Eggers, J., Lister, J. R. and Stone, H. A., *Coalescence of liquid drops.* J. Fluid Mech., 1999. **401**: p. 293-310.
[13] Ashgriz, N. and Poo, J.Y., *Coalescence and separation of binary collisions of liquid drops*. J. Fluid Mech., 1990. **221**: p. 183-204.
[14] Rekvig, L. and Frenkel, D., *Molecular simulations of droplet coalescence in oil/water/surfactant systems.* J. Chem. Phys., 2007. **127**: p. 1-16.
[15] Thoroddsen, S. T., Qian, B., Etoh, T. G. and Takehara, K., *The initial coalescence of miscible drops.* Phys. Fluids, 2007. **19**: p. 1-21.
[16] Mashayek, F., Ashgriz, N., Minkowycz, W. J. and Shotorban, B., *Coalescence collision of liquid drops.* Int. J. Heat Mass Trans., 2003. **46**: p. 77-89.
[17] Xing, X. Q., Butler, D. L., Ng, S. H., Wang, Z., Danyluk, S. and Yang, C., *Simulation of droplet formation and coalescence using lattice Boltzmann-based single-phase model.* J. Coll. Interf. Sci., 2007. **311**: p. 609-618.
[18] Acevedo-Malavé, A. and García-Sucre, M., *3D Coalescence Collision of Liquid Drops using Smoothed Particle Hydrodynamics*. INTECH Publishers, 2011. **5**: p. 85-106.
[19] Monaghan, JJ., *Extrapolating B splines for interpolation*. J. Comput. Phys., 1985. **60**: p. 253-262.
[20] Lucy, L.B., *A numerical approach to the testing of the fission hypothesis*. Astron. J., 1977. **82**: p. 1013-1024.
[21] Gingold, R.A., and Monaghan, JJ., *Smoothed particle hydrodynamics: theory and application to non-spherical stars.* Roy. Astronom. Soc., 1977. **181**: p. 375-389.